0021-972X/07/$15.00/0
Printed in U.S.A.

The Journal of Clinical Endocrinology & Metabolism 92(11):4436–4443

doi: 10.1210/jc.2007-0125

Features of Natural and Gonadotropin-Releasing Hormone Antagonist-Induced Corpus Luteum Regression and Effects of *in Vivo* Human Chorionic Gonadotropin

Felipe Del Canto, Walter Sierralta, Paulina Kohen, Alex Muñoz, Jerome F. Strauss III, and Luigi Devoto

Instituto de Investigaciones Materno Infantil (F.D.C., P.K., A.M., L.D.), Facultad de Medicina, Hospital Clínico San Borja-Arriarán, Universidad de Chile, Santiago 3, Chile; Laboratorio de Ultraestructuras (W.S.), INTA-Universidad de Chile, Santiago 3, Chile; and Department of Obstetrics and Gynecology (J.F.S.), Virginia Commonwealth University School of Medicine, Richmond, Virginia 223298

Context: The natural process of luteolysis and luteal regression is induced by withdrawal of gonadotropin support.

Objective: The objectives of this study were: 1) to compare the functional changes and apoptotic features of natural human luteal regression and induced luteal regression; 2) to define the ultrastructural characteristics of the corpus luteum at the time of natural luteal regression and induced luteal regression; and 3) to examine the effect of human chorionic gonadotropin (hCG) on the steroidogenic response and apoptotic markers within the regressing corpus luteum.

Design: Twenty-three women with normal menstrual cycles undergoing tubal ligation donated corpus luteum at specific stages in the luteal phase. Some women received a GnRH antagonist prior to collection of corpus luteum, others received an injection of hCG with or without prior treatment with a GnRH antagonist.

Main Outcome Measure: Main outcome measures were plasma hormone levels and analysis of excised luteal tissue for markers of apoptosis, histology, and ultrastructure.

Results: The progesterone and estradiol levels, corpus luteum DNA, and protein contents in induced luteal regression resembled those of natural luteal regression. hCG treatment raised progesterone and estradiol in both natural luteal regression and induced luteal regression. The increase in apoptosis detected in induced luteal regression by cytochrome *c* in the cytosol, activated caspase-3, and nuclear DNA fragmentation, was similar to that observed in natural luteal regression. The antiapoptotic protein Bcl-2 was significantly lower during natural luteal regression. The proapoptotic proteins Bax and Bak were at a constant level. Apoptotic and nonapoptotic death of luteal cells was observed in natural luteal regression and induced luteal regression at the ultrastructural level. hCG prevented apoptotic cell death, but not autophagy.

Conclusion: The low number of apoptotic cells disclosed and the frequent autophagocytic suggest that multiple mechanisms are involved in cell death at luteal regression. hCG restores steroidogenic function and restrains the apoptotic process, but not autophagy. **(*J Clin Endocrinol Metab* 92: 4436–4443, 2007)**

THE TERMINAL STAGES of normal luteal regression encompass a loss of functional and structural integrity. Natural luteal regression is characterized by a progressive decline in progesterone (P) biosynthesis, which is associated with a decline in the expression of the steroidogenic acute regulatory protein (StAR) gene and StAR protein levels (1, 2). Furthermore, exogenous human chorionic gonadotropin (hCG) administration to women during the midluteal and late luteal phases results in a significant increase in plasma P as well as StAR gene expression and protein levels within the corpus luteum (3). A decrease in LH levels or a decline in LH receptors does not account for natural luteal regression in primates (4, 5). However, there is a postreceptor loss of LH/hCG signaling efficiency, which is reflected in the high doses of LH/hCG needed to stimulate and sustain the late luteal phase primate corpus luteum (5). Divergent molecular and ultrastructural findings have been reported in the primate corpus luteum during the process of natural luteal regression (6, 7). No changes in the expression of Bcl-2 (8), a cell survival factor, in corpus luteum of different ages has been described, whereas others report a decline in the late luteal phase and an increase in ectopic pregnancy corpus luteum (9). Conversely, expression of the proapoptotic protein Bax has been reported to remain unchanged in the corpus luteum throughout the luteal phase (10) or to increase in late luteal phase (9). Moreover, increasing numbers of apoptotic cells, detected by nuclear DNA fragmentation, in the late luteal phase in regressing corpus luteum, has been described compared with those of early and midluteal phase corpus luteum (11–13).

Therefore, the existing data indicate that apoptosis is a characteristic of natural luteal regression, but the mechanisms that govern it and the relationship between functional and structural regression during luteal rescue in a fertile cycle remain unclear. Withdrawal of LH causes a rapid and profound decline in luteal steroidogenesis and a functional withdrawal of LH action is thought to underlie the natural process of luteolysis. However, it is not yet known whether the structural changes in the luteal cells and their viability contribute to the decline in steroid production that occurs in

First Published Online August 14, 2007

Abbreviations: E2, Estradiol; hCG, human chorionic gonadotropin; P, progesterone; StAR, steroidogenic acute regulatory protein; TdT, terminal transferase; TUNEL, terminal deoxynucleotidyl transferase mediated dUTP nick-end labeling.

JCEM is published monthly by The Endocrine Society (http://www.endo-society.org), the foremost professional society serving the endocrine community.

both the setting of LH withdrawal and functional luteolysis. Moreover, it remains to be determined whether depriving the functional corpus luteum of gonadotropin support mimics the initiation of natural luteal regression. Finally, the extent to which LH and/or hCG modulate the two processes reported to promote luteal cell death, apoptosis, and autophagy, is not known.

Consequently, the aims of this study were: 1) to compare natural luteal regression and induced luteal regression with respect to apoptosis and autophagocytosis and; 2) to determine whether these processes are differentially regulated by hCG.

Subjects and Methods

Subjects and experimental design

The study was approved by the Hospital Clínico San Borja-Arriarán Medical Ethics Committee, and signed informed consent was obtained from all women participating in these studies.

The corpora lutea were enucleated at the time of minilaparotomy for tubal sterilization as described previously (2). The surgery was scheduled at varying times throughout the luteal phase. All women (n = 23) were healthy, aged 33–42 yr, with normal body mass index (kilograms per square meter) and regular menstrual cycles, and they had not received any form of hormonal treatment for at least 3 months before participating in the study. Blood was collected before surgery for P and estradiol (E2) determinations by RIA as previously described (14).

Histological dating of the corpus luteum

The day of ovulation was determined by serial vaginal ultrasound scan and urine LH samples as previously described (2, 3). The corpora lutea were classified as follows: control group: early luteal phase (2–4 d after LH peak; n = 3), midluteal phase (5–9 d after LH peak; n = 4), and late luteal phase (>12 d after LH peak; n = 4); treatment groups: late luteal phase corpus luteum plus hCG (n = 5), midluteal phase corpus luteum plus GnRH antagonist 48 h (n = 4), Midluteal phase corpus luteum plus GnRH antagonist 48 h plus hCG 24 h (n = 3). The entire corpus luteum was enucleated from the ovary under sterile conditions. Tissue for histology and immunodetection was fixed in 4% buffered paraformaldehyde and embedded in paraffin wax. Other pieces were snap-frozen in liquid nitrogen and stored at −70 C for subsequent DNA and protein extraction.

Induced luteal regression and hCG treatment

To induce luteal regression, 2 mg GnRH antagonist (Cetrotide; Serono, Rockland, MA), sc, was administered to women during the midluteal phase (n = 4), and the corpora lutea were collected 48 h after injection. To model luteal rescue, 10,000 IU hCG (Pregnyl; Organon, Oss, The Netherlands), im, was given to women who received GnRH antagonist 48 h before (n = 3) and women during the natural luteal regression (n = 5). Corpora lutea were obtained 24 h after hCG administration.

Cell culture

Luteal cells from midluteal phase corpus luteum (n = 3) were dispersed as previously described (14). The cell viability was more than 90% as assessed by the trypan blue exclusion method. Luteal cells were cultured in serum-free media with GnRH antagonist in doses of 1, 10 and 25 ng/ml in the presence and absence of 10 IU/ml hCG (Sigma Chemical Co., St. Louis, MO) for 24 h. GnRH antagonist doses were chosen according to a previously reported pharmacokinetic study (15). Culture media were collected for P determination.

Protein and DNA quantitation

For protein extraction, luteal tissue was homogenized with a motor-driven glass-Teflon homogenizer in a buffer containing 250 mM sucrose, 30 mM Tris HCl, aprotinin (10 μg/ml), 1 mM phenylmethylsulfonylfluoride, and 50 mM benzamidine. Protein concentration was determined by the dye-binding assay (Bio-Rad Lab. Inc., Hercules, CA). Total DNA was obtained by phenol-chlorophorm extraction followed by ethanol precipitation. Quantitation was carried out by measuring optical density at 260 nm.

Immunodetection of Bcl-2, Bax, and cytochrome c

Western blot analysis of Bcl-2, Bax, and β-actin was performed with whole corpus luteum protein extracts and cytochrome *c* on mitochondria-free supernatants as previously reported (16). Briefly, homogenates were centrifuged first at 600 × *g* for 10 min, and then the supernatant was centrifuged at 12,000 × *g* for 15 min. The mitochondria-rich pellet was discarded. Samples containing 80 μg of protein in the whole extracts and 10 μg of protein in the mitochondria-free supernatant were separated by SDS-PAGE electrophoresis in 12.5% gels and transferred to polyvinylidene difluoride membranes (Hybridon; Millipore Corp., Bedford, MA). To confirm similar loading between samples, the membranes were staining with Ponceau S before hybridization with antibody or reprobed with anti-β-actin. Nonspecific binding sites were blocked with 5% nonfat milk, and membranes were incubated with specific antibodies against Bcl-2 (monoclonal; BD Biosciences, San Diego, CA), Bax (polyclonal; BD Biosciences), and the denaturated form of cytochrome *c* (monoclonal; Zymed Labs, South San Francisco, CA) in 1:2000, 1:1000, and 1:2000 dilutions, respectively. Immunoglobulins were detected using the fluorescent ECF Western Blotting Kit (Amersham Biosciences, Sunnyvale, CA). Images were acquired on a Typhoon 9200 scanner (Amersham Biosciences) and densitometric analysis was performed using ImageQuant 5.2 software (Molecular Dynamics Inc., Sunnyvale, CA).

Light microscopy analysis

Collagen fibers of connective tissue were identified in cryostat sections using a modification of Gomori's trichrome staining (17). Aniline blue and Harris hematoxylin were used instead of light green and of iron-hematoxylin respectively. Apoptotic cells were identified in hematoxylin/eosin-stained paraffin sections of tissue based on morphological characteristics including cell shrinkage, acidophilic cytoplasm, and pyknosis. Images from a standard light microscope were acquired with the Cool-SNAP-Pro Color ccd camera system and analyzed with Image ProPlus 4.5 software (Media Cybernetics, Silver Spring, MD).

Detection of active caspase 3 by immunofluorescence

Immunodetection of active caspase 3 was performed on 5-μm tissue sections mounted on silanized slides. Briefly, paraffin sections were dewaxed with a xylene substitute (Polyclear solvent; Polysciences, Warrington, PA) and rehydrated in a graded series of ethanol. Antigen retrieval was performed by heating at 95 C in 10 mM glycine, pH 6.0. After blocking with 1% BSA in PBS, sections were incubated with a monoclonal antibody that recognizes specifically the active form of caspase 3 (BD Biosciences) in a 1:100 dilution. After washing, sections were incubated with an antirabbit IgG conjugated to Alexa-488 (Molecular Probes). Nuclei were counterstained with 1 μg/ml propidium iodide, and slides were mounted using fluorescent mounting medium (Dako, Carpinteria, CA). Images were acquired from an Olympus BX51 fluorescence microscope fitted with the ccd-color camera described above.

Terminal deoxynucleotidyl transferase mediated dUTP nick-end labeling (TUNEL) assay

Apoptotic cells were detected using the TUNEL method, following the manufacturer instructions (Promega, Madison, WI). Briefly, dewaxed tissue sections were rehydrated, fixed, permeabilized with 10 ng/ml proteinase K, and incubated in the dark for 1 h at 37 C with terminal transferase (TdT) in the presence of fluorescent nucleotides (dUTP-FITC). Negative controls were slides incubated without TdT. The nuclei were stained with 1 μg/ml propidium iodide. TUNEL-positive cells were counted in 20 randomly selected fields; the results were expressed as number of apoptotic cells per total area of 1.3 mm^2.

Ultrastructural analysis

Fragments of corpus luteum, approximately 1 mm^3, were fixed overnight by immersion in 2.5% (wt/vol) glutaraldehyde prepared in 0.1 M phosphate buffer, pH 7.4. Samples were washed with phosphate buffer, postfixed with 0.25% osmium tetroxide, dehydrated with graded acetone solutions, and embedded in epoxy as previously described (17). Ultrathin sections were cut from the blocks using a Reichert-Jung ultramicrotome. The sections were collected on 200 mesh grids, poststained with 5% aqueous uranyl acetate and Reynolds lead citrate, inspected with a Philips CM100 electron microscope at 80 kV (Phillips, Eindhoven, The Netherlands), and photographed on Kodak 4489 EM film (Kodak, Rochester, NY).

Statistical analysis

The results were analyzed by one-way ANOVA followed by Tukey's multiple comparison test (GraphPad Prism version 4.5.1; GraphPad Software, San Diego, CA). Data are expressed as mean ± SEM. P values < 0.05 were considered significant.

Results

Description of corpus luteum and plasma steroid hormone levels throughout the luteal phase, induced luteal regression, and after hCG administration

Table 1 summarizes changes in corpora lutea weight, protein content, DNA content, and plasma concentrations of LH, P, and E2 at the different stages of the luteal phase. A significant decrease in protein content was only observed in natural luteal regression. LH plasma concentrations were significantly reduced in Cetrotride-treated women. As expected, plasma concentrations of both P and E2 were lower in natural luteal regression and induced luteal regression than during the early and midluteal phases. The administration of hCG in the midluteal and late luteal phase, to women previously treated with Cetrotide resulted in higher plasma E2 and P concentrations than those found in natural luteal regression and induced luteal regression. The concentration of E2 and P in plasma after hCG stimulation in natural luteal regression and induced luteal regression reached similar levels to those found at the midluteal phase. Thus, the ovarian response in terms of E2 and P secretion was similar in natural luteal regression and induced luteal regression.

Morphological characteristics of luteal regression

The corpus luteum undergoes significant structural changes during natural luteal regression and induced luteal regression. These changes occur concurrently with decreased endocrine function of the corpus luteum. Figure 1A depicts the redistribution of connective tissue throughout the corpus luteum in concert with shrinkage of large luteal cells in the late luteal phase. The midluteal phase corpus luteum shows a peripheral distribution of connective tissue with the presence of some connective tissue between steroidogenic cells. Corpora lutea obtained in the setting of induced luteal regression showed a peripheral distribution of connective tissue despite the reduction of total weight similar to the midluteal phase corpus luteum. Figure 1B shows the percentage of area corresponding to connective tissue (blue staining in panel A), in midluteal phase corpus luteum, natural luteal regression, and induced luteal regression. The area occupied by connective tissue is significantly larger in natural luteal regression ($P < 0.05$) than midluteal phase corpus luteum and induced luteal regression.

Effect of GnRH antagonist on cultured luteal cells

Figure 2 shows the effect of different doses of GnRH antagonist on P accumulation by cultured midluteal phase cells in the presence and absence of hCG. Cultures treated with 10 IU/ml hCG for 24 h accumulated higher amounts of P than control (no treatment) and than GnRH antagonist ($P < 0.05$). GnRH antagonist treatment did not affect hCG-stimulated production of P by cultured luteal cells. These data indicate that these doses of GnRH antagonist do not have a direct effect on luteal P production *in vitro*.

Cytochrome c and active caspase 3

Figure 3A presents a representative Western blot for cytochrome *c* showing an immunoreactive band at 12 kDa that increased progressively throughout the luteal phase and after GnRH antagonist administration. natural luteal regression and induced luteal regression displayed the highest abundance of cytosol cytochrome *c*. The densitometric analysis illustrates the relative abundance of cytochrome *c* being 3- and 2-fold greater in natural luteal regression and induced luteal regression, respectively. hCG administration at the time of natural luteal regression and induced luteal regression decreased significantly the relative abundance of cytochrome *c* in the postmitochondrial supernatant ($P < 0.05$).

TABLE 1. Characteristics of corpus luteum (CL) and plasma hormone levels throughout the luteal phase and ILR, and after hCG administration

	Early	Mid	NLR	NLR + hCG	ILR	ILR + hCG
CL weight (g)	1.12 ± 0.21	1.58 ± 0.14	0.83 ± 0.18[a]	1.55 ± 0.18	0.92 ± 0.17[a]	1.16 ± 0.34
Proteins (mg/100 mg tissue)	11.52 ± 1.88	6.63 ± 0.74	4.57 ± 1.05[b]	8.18 ± 1.22	5.65 ± 1.15	7.40 ± 1.57
DNA (μg/100 mg tissue)	234.9 ± 45	234.5 ± 67	197.2 ± 22	236.8 ± 43	201 ± 37	349 ± 67
LH (UI/liter)	6.70 ± 1.1	5.98 ± 2.1	2.87 ± 0.5		1.42 ± 0.2[c]	
P (nmol/liter)	34.0 ± 7.4	37.7 ± 4.0	8.1 ± 3.2[d]	34.0 ± 8.0	9.5 ± 4.8[d]	33.6 ± 6.1
E2 (pmol/liter)	665 ± 66	549 ± 81	327 ± 67	531 ± 105	238 ± 38[e]	477 ± 110

Values are the mean ± SEM. Statistical analysis: ANOVA followed by Tukey test. NLR, Natural luteal regression; ILR, induced luteal regression.

[a] $P < 0.05$ *vs.* mid CL.
[b] $P < 0.05$ *vs.* early CL.
[c] $P < 0.05$ *vs.* early and midluteal phase.
[d] $P < 0.05$ *vs.* early and midluteal phase.
[e] $P < 0.05$ *vs.* early and mid luteal phase.

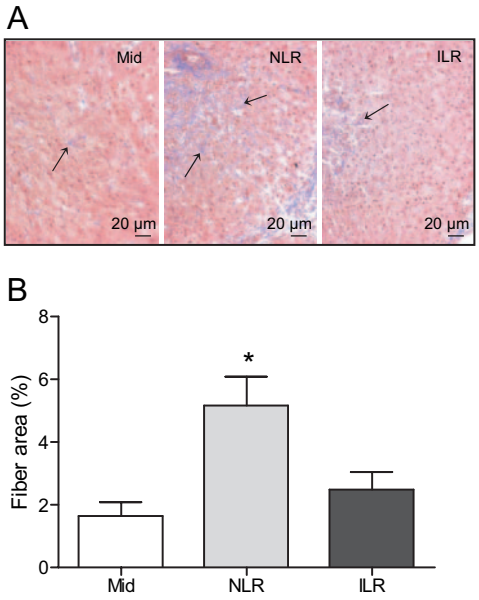

FIG. 1. Distribution of connective tissue in midluteal phase corpus luteum (Mid), natural luteal regression (NLR) and induced luteal regression (ILR). A, A *blue*-stained connective tissue (*black arrow*), *red*- stained cytoplasm, and more intensely stained nuclei. B, Percentage of area occupied by connective tissue (visual field 0.26 mm^2). Values are the mean ± SEM from 44 visual fields examined. *, $P < 0.05$, compared with midluteal phase corpus luteum and induced luteal regression.

Figure 3B depicts the immunodetection of the active form of caspase 3, a key effector protease involved in the apoptotic cascade. The protein was detected by immunofluorescence (number of cells × 1.3 mm^2) in tissue sections of midluteal phase corpus luteum (25 ± 4), natural luteal regression (76 ± 8), induced luteal regression (76 ± 10), and hCG-stimulated corpus luteum of both natural (19 ± 5) and induced luteal regression (26 ± 4). In all cases, immunostaining was observed in the cytoplasmatic compartment of the luteal cells. Tissue sections incubated without the anti-caspase 3 antibody served as a negative control. Few immunopositive cells were observed in midluteal phase corpus luteum, suggesting that the apoptotic process may be initiated at a later stage. Corpora lutea collected during natural luteal regression or induced luteal regression showed an increasing number of

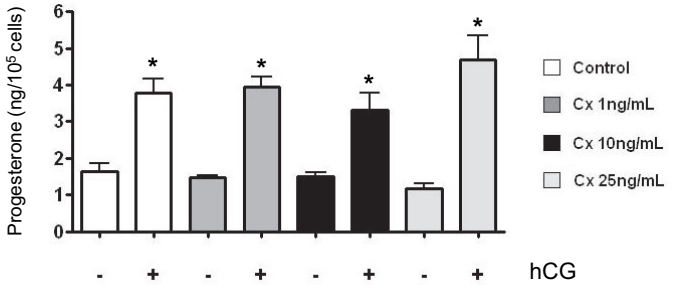

FIG. 2. Effect of GnRH antagonist (Cx) on P production by midluteal cells. The cells were cultured for 24 h in the absence (control) or presence of hCG (10 IU/ml) and GnRH antagonist (0, 1, 10, and 25 ng/ml). Values are mean ± SEM from four individual corpora lutea. *, $P < 0.05$ compared with control.

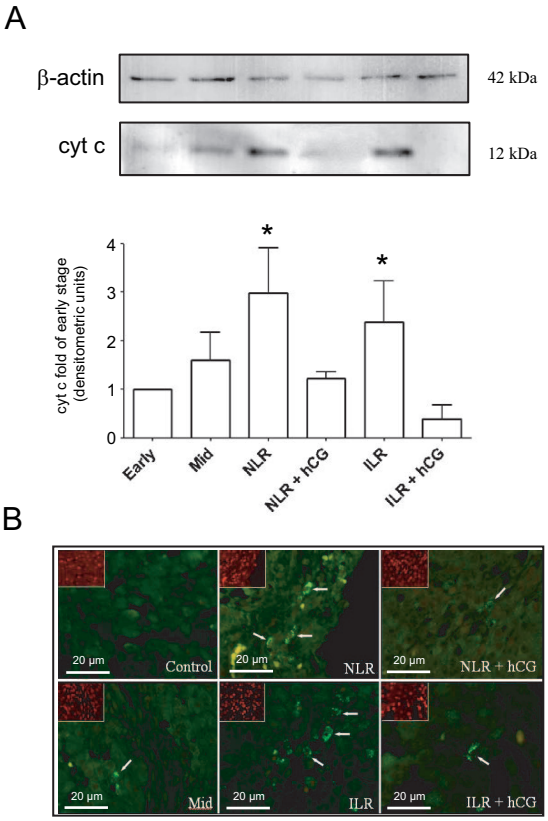

FIG. 3. Apoptosis during luteal regression. A, Western blot and densitometric analysis for cytochrome *c* in postmitochondrial supernatants of corpus luteum obtained during early and midluteal phases, natural luteal regression (NLR), induced luteal regression (ILR), and 24 h after hCG administration at natural luteal regression and induced luteal regression. Densitometric results are expressed as fold of the early luteal phase corpus luteum and normalized by β-actin detection. Values are mean ± SEM from three individual corpora lutea. *, $P < 0.05$ compared with all. B, Active caspase 3 detection by indirect immunofluorescence (*white arrows*). Control, tissue incubated without primary antibody. *Inset panels* show nuclear staining with propidium iodide.

immunopositive cells ($P < 0.05$). hCG administration to women during natural luteal regression or induced luteal regression, resulted in a decrease in the number of active caspase 3 immunopositive cells.

DNA fragmentation (TUNEL)

Figure 4 illustrates apoptotic luteal cells detected by light microscope examination (panel A) of hematoxylin/eosin tissue sections. The typical features of apoptosis including an acidophilic cytoplasm, pyknosis, and cell shrinkage are observed. *In situ* detection of nuclear DNA fragmentation is shown in Fig. 4B. The number of cells showing positive fluorescence nuclear staining in midluteal phase cells was limited (Fig. 4C). Conversely, natural luteal regression and induced luteal regression were associated with a greater number of apoptotic cells compared with midluteal phase corpus luteum. hCG treatment of women during natural luteal regression and induced luteal regression resulted in a significant decrease in the number of apoptotic cells ($P < 0.05$).

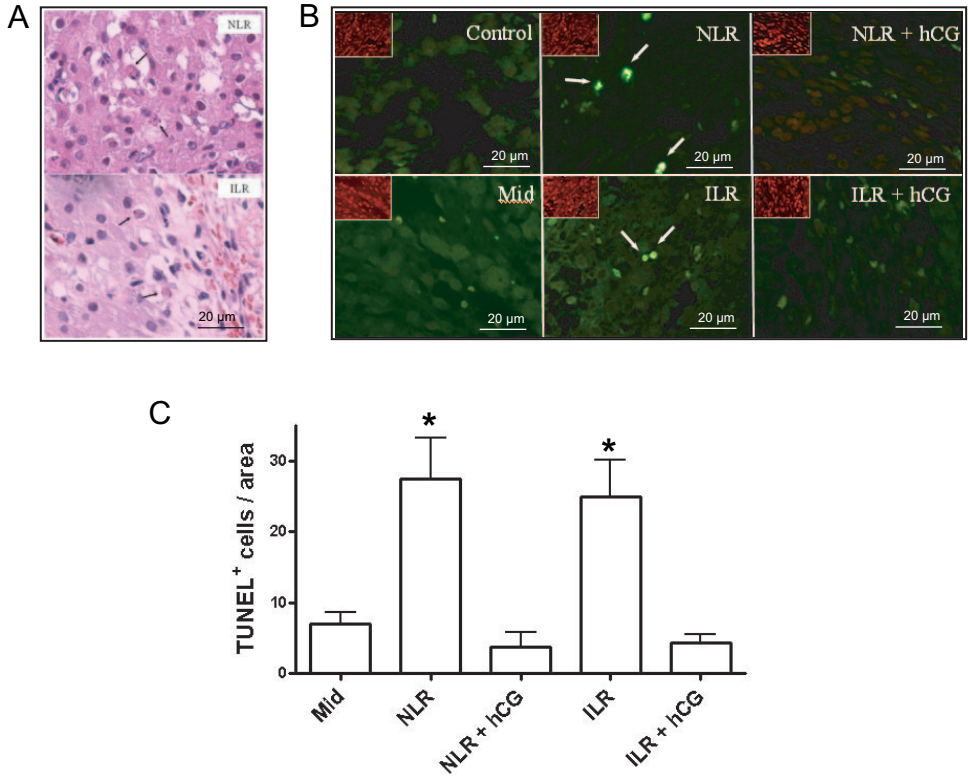

FIG. 4. Morphological evidence for apoptosis during luteolysis. A, The apoptotic cells in hematoxylin/eosin-stained tissue sections of corpus luteum obtained during natural luteal regression (NLR) and induced luteal regression (ILR) (*black arrows*). B, *In situ* detection of nuclear DNA fragmentation by TUNEL (*white arrows*). Control, tissue incubation without TdT. *Inset panels* show nuclear staining with propidium iodide. C, The quantitation of apoptotic cells detected by TUNEL. Positively stained cells were counted on 20 visual fields randomly selected (total area = 1.3 mm^2). Values represent the mean ± SEM from four individual corpora lutea. *, $P < 0.05$ significantly different than mid, natural luteal regression plus hCG, and induced luteal regression plus hCG.

Bcl-2 and Bax in the corpus luteum

Figure 5 is a representative Western blot analysis of the classic antiapoptotic regulatory proteins in the corpus luteum. The blot shows immunoreactive bands of β-actin at 42 kDa, bcl-2 at 26 kDa, and Bax at 21 kDa. The abundance of Bcl-2 was significantly lower in natural luteal regression compared with early and midluteal phase tissue ($P < 0.05$). GnRH antagonist administration in the midluteal phase reduced the Bcl-2 protein expression. However, the decline was not statistically significant. Administration of hCG reestablished the Bcl-2 signal in both types of luteal regression. The densitometric analysis of Bax revealed a constant level of expression throughout the luteal phase. Interestingly, neither GnRH antagonist nor hCG changed the pattern of Bax protein expression. These data suggest that the expression of Bcl-2 protein is age- and hCG-dependent, whereas the expression of Bax protein is not.

Ultrastructural characteristics of the corpus luteum

Figure 6 shows representative photomicrographs from ultrathin sections of human corpus luteum obtained during the midluteal phase (panel A), natural luteal regression (line B), induced luteal regression (panels C and D), and natural luteal regression plus hCG (panel E). Luteal cells from midluteal phase corpus luteum have characteristic lipid droplets and intact nuclei and mitochondria. Extensive vacuolization of the cytoplasm appears in granulosa-lutein cells during both types of regression. The presence of autophagosomes containing incompletely digested material point to autophagocytosis as a process that is relevant in natural luteal regression. Phagocytic structures were also present in corpus luteum obtained during induced luteal regression, supporting the idea that the administration of GnRH antagonist activates nonapoptotic degeneration of human luteal cells. Midluteal and late luteal phase corpus luteum collected 48 h after hCG administration did not show a reduction in autophagocytosis. However, mitochondria were increased in size, appearing swollen, but with an intact-appearing mitochondrial membrane.

Discussion

At the end of a nonfertile cycle, the corpus luteum of many species undergoes a dynamic process of regression known as luteolysis which includes functional changes, particularly a decline in P production, and structural changes including apoptosis, necrosis, and autophagocytosis (7, 11, 18, 19). This study reappraised simultaneously the functional and structural regression of the human corpus luteum, luteolysis induced by administration of GnRH antagonist, and a model of corpus luteum rescue with administration of hCG.

The weight of the gland and its protein content decreased significantly throughout the luteal phase. This is presumably related to the postreceptor loss of LH signaling efficiency in late luteal phase corpus luteum, and the consequence of the significant decrease in LH secretion in Cetrotide-treated women. Interestingly, connective tissue occupied a significantly larger area of the corpus luteum medulla in natural luteal regression, in comparison to induced luteal regression and the midluteal phase corpus luteum. These data do not necessarily mean that production of connective tissue fibers

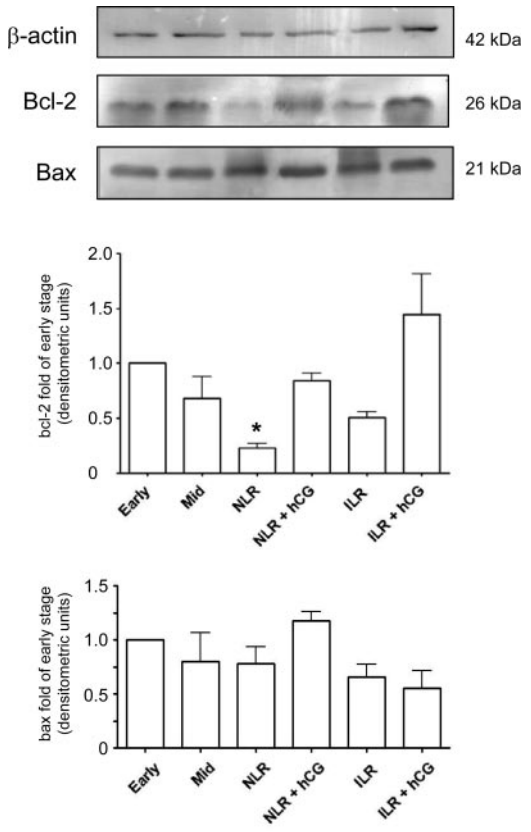

FIG. 5. Expression of antiapoptotic and proapoptotic proteins in the human corpus luteum. Representative Western blot of β-actin, Bcl-2, and Bax. Densitometric histograms are expressed as fold of the early luteal phase, normalized by β-actin detection. Values are mean ± SEM for at least three different corpora lutea in each experimental group. Luteal Bcl-2 in natural luteal regression is significantly different (*, $P < 0.05$) compared with early luteal phase corpus luteum. Bax did not exhibit significant changes.

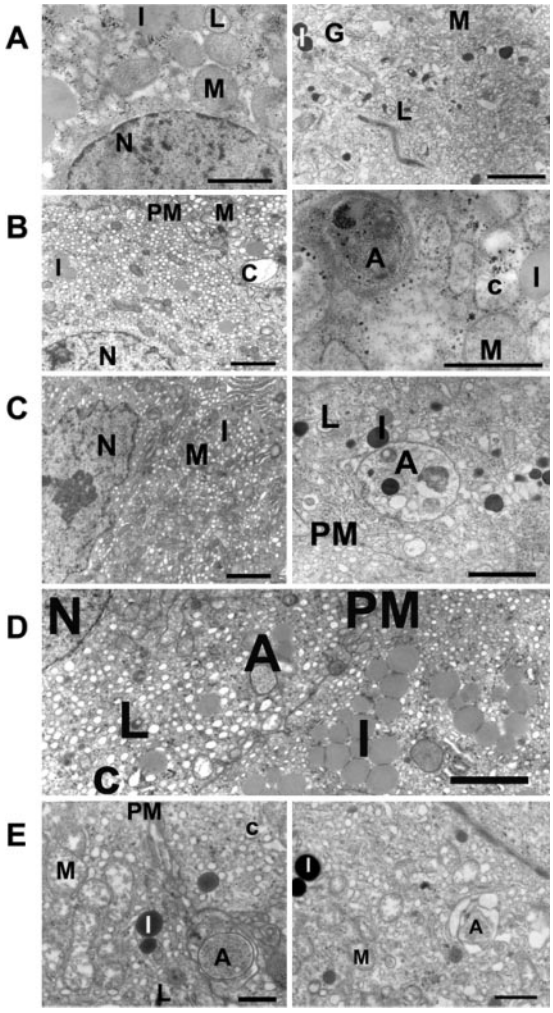

FIG. 6. Ultrastructural features of luteolysis. Photomicrographs showing ultrastructural aspects of corpus luteum cells. A, Corpus luteum obtained during midluteal phase; B, natural luteal regression; C and D, induced luteal regression; and E, late luteal phase plus hCG. For all: N, nucleus; M, mitochondrion; C, cisternae of endoplasmic reticulum; l, lipid droplets; L, lysosome; A, autophagosome; PM, plasma membrane; G, Golgi apparatus. The *bar* represents 1 μm in A *left*, B *right*, and E *right*; and in all others, 2 μm.

increased during natural luteal regression, but might represent a redistribution of connective tissue, that together with shrinkage of all cell layers and the loss of extracellular matrix components, results in a relatively larger area of this matrix in the observed microscopic fields. These microscopic observations are consistent with a recent study of luteal ultrasound echogenicity during luteal development, in association with increased P and E2 serum concentrations (20). Decreased echogenicity during luteinization suggests increased vascularization of luteal tissue and a corresponding decrease in tissue density. In contrast, the increased echogenicity described during the late luteal phase could be attributed to decreased vascularization and replacement of luteal tissue with connective tissue (21).

In the present study, the molecular appraisal of apoptosis shows that cytochrome *c* is released progressively from mitochondria into the cytosol of cells throughout the luteal phase. The administration of hCG reduced the abundance of cytochrome *c* in the cytosol of luteal cells from both natural luteal regression and in induced luteal regression. It has been previously reported that hCG causes hyperpolarization of the mitochondrial transmembrane potential ($\rho\psi_m$) protecting human granulosa cells from ATP-induced apoptosis (22). Protective effects of hCG on corpus luteum apoptosis were revealed also by the reduction in the caspase 3 activation and DNA fragmentation that resulted in a significant decrease in the number of apoptotic luteal cells in both types of corpus luteum regression. These findings suggest that the diminished signaling of LH in late luteal cells or the acute reduction of plasma LH induced by GnRH antagonist triggers the apoptotic process.

Our data confirm previous reports that Bcl-2 protein decreases significantly in natural luteal regression in comparison to early and midluteal phase corpus luteum tissue, but that was not the case for induced luteal regression (9). This divergence presumably reflects different molecular mechanisms involved in natural and induced luteal regression. Conversely, Bax remained constant in corpus luteum of different ages and in natural luteal regression and induced luteal regression. Furthermore, we examined the proapop-

totic proteins Bak and Bok (data not shown); these proteins are expressed in the human corpus luteum, but their expression is not age-dependent. hCG administration at the time of natural luteal regression and induced luteal regression caused an increase in Bcl-2, but the effect on proapoptotic protein Bax, was variable, and not hCG-dependent, and thus difficult to reconcile according to their known roles in the apoptotic process. Overall, our results suggest that hCG protects luteal cell viability at different levels: 1) by diminishing cytochrome *c* release, 2) reducing caspase 3 activation, 3) up-regulating Bcl-2 protein, and 4) possibly increasing other survival factors.

The expression of GnRH and GnRH-receptors in the human ovary has been reported (23). Therefore, a direct effect of GnRH antagonist on luteal cells cannot be excluded. However, this seems to be unlikely because our experiments using high doses of GnRH antagonist did not show interference with P production by luteal cells *in vitro*. Additionally, there was no change in the *in vivo* production of P stimulated by hCG of corpus luteum previously treated with GnRH antagonist (3).

There is no doubt that apoptosis is a component of the complex process of luteal regression in women. However, the low number of luteal cells exhibiting apoptosis may suggest that this process is not the only mechanism of cell death in the human corpus luteum. Previous ultrastructural studies have demonstrated in the marmoset that different forms of luteal degeneration and cell death contribute to the process of natural luteal regression. Fraser *et al.* (7, 24) postulated that, during natural or induced luteolysis, the vast majority of primate luteal cells died by nonapoptotic mechanisms, including autophagocytosis and necrosis. Currently, autophagocytosis is considered an emergency mechanism for survival under stress conditions like starvation (25). Thus, a cell undergoing autophagocytosis would finally die by apoptosis or necrosis.

As judged from the plasma membrane condition, the swelling of mitochondria, the apparent preservation of the nucleus, and minor changes in other organelles, cell death by necrosis was occasionally observed in the corpus luteum samples. In very few cells, chromatin compaction toward the nuclear periphery was seen, pointing to a limited occurrence of apoptosis. In dozens of sections from embedded natural luteal regression corpus luteum, the remains of cells were in close approximation to phagocytes, indicating that late apoptotic events occur with low frequency. A more commonly found indication of cell death was the presence inside many corpus luteum cells of multisided, double-membrane outlined organelles, usually containing copious amounts of nondigested material (autophagosomes).

In the present study, we found that apoptosis in the corpus luteum during natural luteal regression/induced luteal regression is not a prominent process. This could reflect a limited role for apoptosis in luteolysis, or kinetics in which apoptotic cells are rapidly cleared, leaving the impression of an infrequent event. The electron microscope studies detected autophagocytosis in both types of regressing corpus luteum, suggesting that this is a more important mode of cell death during luteolysis, or that its kinetics are much slower than that of apoptotic demise. hCG administration during the midluteal phase restrains the apoptotic process but was ineffective in preventing the ultrastructural characteristics of autophagocytosis. Interestingly, our study demonstrated healthy mitochondria with preservation of the mitochondrial membrane structure, which may account for the retained capacity of corpus luteum to respond with increased steroidogenesis to hCG in the late luteal phase.

In conclusion, our findings indicate that luteal cell shrinkage, with different types of cell degeneration and death, account for the loss of weight of the corpus luteum during luteal regression. These structural, molecular, and ultrastructural data indicate a reduction in protein content of luteal tissue with biochemical and morphological markers indicating active apoptotic and autophagocytosis processes during luteal regression and that the mechanisms leading to natural luteal regression and induced luteal regression are different. However, they do not hamper the response of the corpus luteum to hCG, suggesting that the capacity for response to an acute hCG stimulus is preserved, at least in the initial stages of both types of luteal regression. Therefore, information on the significance of the key proapoptotic and antiapoptotic proteins, during corpus luteum development, function, demise, and rescue by hCG is likely to bring new therapeutic applications for the management of fertility defects and control of fertility.

Acknowledgments

We thank Verónica Alam, M.D., Medical Director, Serono Geneva, Switzerland for providing Cetrotide, Cetrorelix acetate.

Received January 17, 2007. Accepted August 8, 2007.

Address all correspondence and requests for reprints to: Luigi Devoto, M.D., Faculty of Medicine, University of Chile, P.O. Box 226-3, Santiago, Chile. E-mail: ldevoto@med.uchile.cl.

This work was supported by grants from the Chilean Research Council (Comisión Nacional de Investigación Científica y Technologica-Fondos Nacional de Desarrollo Areas Prioritarias no. 15010006), and the National Institutes of Health (HD06274, Fogarty Center, Fogarty International Research Collaboration Award, and National Institutes of Health Fogarty 5D43TW007692).

Disclosure Statement: The authors have nothing to declare.

References

1. **Christenson LK, Devoto L** 2003 Cholesterol transport and steroidogenesis by corpus luteum. Reprod Biol Endocrinol 1:90
2. **Devoto L, Kohen P, Gonzalez R, Castro O, Retamales I, Vega M, Carvallo P, Christenson LK, Strauss III JF** 2001 Expression of steroidogenic acute regulatory protein in the human corpus luteum through the luteal phase. J Clin Endocrinol Metab 86:5633–5639
3. **Kohen P, Castro O, Palomino A, Muñoz A, Christenson L, Sierralta W, Carvallo P, Strauss III JF, Devoto L** 2003 The steroidogenic response and corpus luteum expression of the steroidogenic acute regulatory protein alter human chorionic gonadotropin administration at different times in the human luteal phase. J Clin Endocrinol Metab 88:3421–3430
4. **Duncan WC, McNelly AS, Fraser HM, Illingworth PJ** 1996 Luteinizing hormone receptor in the human corpus luteum: lack of down-regulation during maternal recognition of pregnancy. Hum Reprod 11:2291–2297
5. **Zeleznik A** 1998 In vivo responses of the primate corpus luteum to luteinizing hormone and chorionic gonadotropin. Proc Natl Acad Sci USA 95:11002–11007
6. **Gaytán F, Morales C, García-Pardo L, Reymundo C, Bellido C, Sánchez-Criado JE** 1998 Macrophages, cell proliferation, and cell death in the human menstrual corpus luteum. Biol Reprod 59:417–425
7. **Fraser HM, Lunn SF, Harrison DJ, Kerr JB** 1999 Luteal regression in the primate: different forms of cell death during natural and gonadotropin-releasing hormone antagonist or prostaglandin analogue-induced luteolysis. Biol Reprod 61:1468–1479
8. **Rodger FE, Fraser HM, Duncan WC, Illingworth PJ** 1995. Cell cycle: immu-

nolocalization of Bcl-2 in the human corpus luteum. Hum Reprod 10:1566–1570
9. **Sugino N, Suzuki T, Kashida S, Karube A, Takiguchi S, Kato H** 2000 Expression of Bcl-2 and Bax in the human corpus luteum during the menstrual cycle and in early pregnancy: regulation by human chorionic gonadotropin. J Clin Endocrinol Metab 85:4379–4386
10. **Rodger FE, Fraser HM, Krajewski S, Illingworth PJ** 1998 Production of the proto-oncogene BAX does not vary with changing in luteal function in women. Mol Hum Reprod 4:27–32
11. **Shikone T, Yamoto M, Kokawa K, Yamashita K, Nishimori K, Nakano R** 1996 Apoptosis of human corpora lutea during cyclic luteal regression and early pregnancy. J Clin Endocrinol Metab 81:2376–2380
12. **Yuan W, Giudice LC** 1997 Programmed cell death in human ovary is a function of follicle and corpus luteum status. J Clin Endocrinol Metab 82:3148–3155
13. **Vaskivuo TE, Ottander U, Oduwole O, Isomaa V, Vihko P, Olofsson JI, Tapanainen JS** 2002 Role of apoptosis, apoptosis-related factors and 17β-hydroxysteroid dehydrogenases in human corpus luteum regression. Mol Cell Endocrinol 194:191–200
14. **Devoto L, Kohen P, Castro O, Vega M, Troncoso JL, Charreau E** 1995 Multihormonal regulation of progesterone synthesis in cultured human midluteal cells. J Clin Endocrinol Metab 80:1566–1570
15. **Duijkers IJM, Klipping C, Willemsen WNP, Krone D, Schneider E, Niebch G, Hermann R** 1998 Single and multiple dose pharmacokinetics and pharmacodynamics of the gonadotropin-releasing hormone antagonist Cetrorelix in healthy female volunteers. Hum Reprod 13:2392–2398
16. **Gomori, GL** 1950 A rapid one-step trichrome stain. Amer J Clin Path 20:661–664
17. **Sierralta WD, Kohen P, Castro O, Muñoz A, Strauss III JF, Devoto L** 2005 Ultrastructural and biochemical evidence for the presence of mature steroidogenic acute regulatory protein (StAR) in the cytoplasm of human luteal cells. Mol Cell Endocrinol 242:103–110
18. **Morales C, García-Pardo L, Reymundo C, Bellido C, Sánchez-Criado JE, Gaytán F** 2000 Different patterns of structural luteolysis in the human corpus luteum of menstruation. Hum Reprod 15:2119–2128
19. **Stocco C, Tellerías C, Gibori G** 2007 The molecular control of corpus luteum formation, function and regression. Endocr Rev 28:117–149
20. **Baerwald AR, Adams GP, Pierson RA** 2005 Form and function of the corpus luteum during the human menstrual cycle. Ultrasound Obstet Gynecol 25:498–507
21. **Glock J, Brumsted J** 1995 Color flow pulsed Doppler ultrasound in diagnosing luteal phase defect. Fertil Steril 64:500–504
22. **Park DW, Cho T, Kim MR, Kim YA, Min CK, Hwang KJ** 2003 ATP-induced apoptosis of human granulosa luteal cells cultured in vitro. Fertil Steril 80:993–1002
23. **Ramakrishnappa N, Rajamahendran R, Lin Y, Leung PCK** 2005 GnRH in non-hypothalamic reproductive tissues. Anim Reprod Sci 88:95–113
24. **Fraser HM, Lunn SF, Cowen GM, Illingworth PJ** 1995 Induced luteal regression in the primate: evidence for apoptosis and changes in c-*myc* protein. J Endocrinol 147:131–137
25. **Baehrecke EH** 2005 Autophagy: dual roles in life and death. Nat Rev Mol Cell Biol 6:505–510

JCEM is published monthly by The Endocrine Society (http://www.endo-society.org), the foremost professional society serving the endocrine community.